Photochemistry and Photobiology, 2015, 91: 1324–1331

Photoisomerization of *Trans Ortho*-, *Meta*-, *Para*-Nitro Diarylbutadienes: A Case of Regioselectivity

Harsha Agnihotri, Mahalingavelar Paramasivam, Veerabhadraiah Palakollu and Sriram Kanvah*

Department of Chemistry, Indian Institute of Technology Gandhinagar, Ahmedabad, India

Received 4 May 2015, accepted 12 July 2015, DOI: 10.1111/php.12504

ABSTRACT

A series of *ortho*-, *meta*- and *para*-substituted *trans*-nitro aryl (phenyl and pyridyl) butadienes have been synthesized and characterized. The effect of substitution and positional selectivity on their fluorescence and photoisomerization were systematically investigated. Among all dienes, *meta*- and *para*-nitro phenyl-substituted derivatives exhibit remarkable solvatochromic emission shifts due to intramolecular charge transfer. On the other hand, *ortho* derivatives undergo regioselective isomerization upon photoexcitation in contrast to inefficient isomerization of *para* and *meta* nitro-substituted dienes. Single crystal X-ray analysis revealed existence of intramolecular hydrogen bonding between the nitro group and the hydrogen of the proximal double bond. This restricts the rotation of the proximal double bond thereby allowing regioselective isomerization. The observations were also supported by NMR spectroscopic studies.

INTRODUCTION

Photoinduced isomerization of the double bond plays a vital role for many biologically relevant pigments such as the opsin family of proteins (1–3). The energy level proximities of diphenylpolyenes in comparison to the retinylidene polyenes led to their use as model compounds toward examination of photoisomerization reactions (4) as well for mechanistic considerations (5–9). Coupled with their biological relevance, the emission and photoswitchable properties of such arylethylene derivatives have found use for biological (10) and optical electronic applications (11,12). In particular, suitably substituted π-conjugated derivatives bearing different functional groups exhibiting intramolecular charge transfer (ICT) have found applicability as functional materials (13,14), as fluorescence probes (15–18), for optical applications (19–21) and to understand substituent dependent photochemical and photophysical processes (22–24). Common to some of these known materials is presence of the nitro group as an acceptor moiety despite it being accounted for efficient nonradiative transitions such as internal conversion and intersystem crossing processes. The preference for electron withdrawing nitro group is due to its profound influence on emission characteristics, owed to the existence of ICT or twisted intramolecular charge transfer states (25–27), and its influence on photochemistry due to involvement of triplet excited states (28). Aside from phenyl-substituted conjugated derivatives, push-pull-substituted heteroaryl containing derivatives were also investigated (29). For instance, replacing the CH group by nitrogen (N) in the phenyl ring yields an isoelectronic heteroaryl species that can significantly change the observed photophysical properties (30). Many of these isoelectronic pyridyl stilbenes and dienes have been synthesized and their excited state properties were investigated (31–34). Mechanistic studies of isomerization of these diphenyl or diarylpolyenes led to a wholesome debate over isomerization mechanisms (6–9). In this report, we discuss the photoinduced behavior (fluorescence and photoisomerization) of different positional [*ortho (o-)*, *meta (m-)* or *para (p-)*] isomers of nitro diarylbutadienes (Fig. 1). We expect that changing the position of the nitro group will influence the electron delocalization and in turn affect the photochemical and fluorescence properties. The results reveal that in case of phenyl-substituted derivatives, *p*- and *m*-substitution leads to fluorescence characterized by intramolecular charge transfer (ICT), whereas *o*-derivatives quench the fluorescence. Upon replacing phenyl with pyridine, *p*-derivative leads to ICT, *m*-substitution results in quenching with weak long wavelength bands, whereas no ICT characteristics were seen for *o*-nitro substitution. Photochemical studies indicate *o*-substitution has maximum impact on photoisomerization while *m*- and *p*-derivatives exhibit inefficient isomerization in both phenyl- and pyridyl-substituted dienes. The results are detailed in the following sections.

MATERIALS AND METHODS

The reagents required for the synthesis of diene derivatives were obtained from chemical vendors such as Sigma-Aldrich, Alfa Aesar, Acros, S.D Fine and Spectrochem. The solvents needed for the synthesis and spectral studies were dried using established procedures. ^{1}H and ^{13}C NMR spectra were carried out in $CDCl_3$ with tetramethylsilane as internal standard using 500 MHz Bruker Avance spectrometer. Accurate mass analysis was performed using Waters-Synapt G2S (ESI-QToF) mass spectrometer. Absorption spectra were recorded on Analytikjena, Specord 210 model UV–vis spectrophotometer. High pressure liquid chromatography (HPLC) was performed using Agilent 1260 infinity fitted with Kinetex 5μ C18 100 Å (250 × 4.6 mm) column. Acetonitrile-water mixture (50–60%) with a flow rate of 1.0 mL min^{-1} is used as eluent for all the samples. The monitoring wavelengths for detecting the photoproducts are 315 nm (for diene **6**), 320 nm (for **3**), 330 nm (for **2** & **5**) and 370 nm (for **1** & **4**). Steady-state fluorescence studies were performed utilizing Horiba Jobin Yvon fluorolog-3 spectrofluorimeter and relative fluorescence quantum yields were measured using quinine sulfate (0.545 in 0.5 N H_2SO_4) as standard (35). The concentrations used for fluorescence experiments are in the order of 10^{-5} M. Typically, the excitation wavelengths were set at the absorption maxima (λ_a) of the compounds under investigation. For photochemical irradiation experiments, a sample (3 mL of ~10^{-5} M) in acetonitrile was

---

*Corresponding author email: kanvah@gmail.com (Sriram Kanvah)

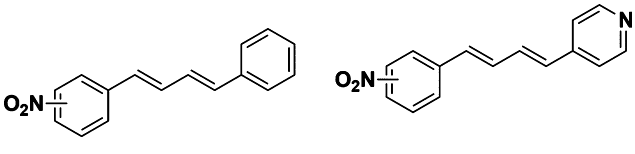

p- (**1**), *m*- (**2**), *o*- (**3**) *p*- (**4**), *m*- (**5**), *o*- (**6**)

Figure 1. Structures of dienes investigated.

performed in a 1 cm path length quartz cuvette and irradiated using 125 W medium pressure Hg vapor lamp. Ten percent copper sulfate pentahydrate solution having 100% transmittance from 330 to 560 nm was chosen as the cut-off solution filter. Progress of the irradiation was monitored using UV–visible spectroscopy and HPLC. For characterization purposes, a higher concentration of sample solutions (3 mg in 1 mL of $CDCl_3$) was irradiated for 2 hours using 125 W medium pressure Hg lamp. Quantum yields of photoisomerization (ϕ_{PI}) were performed using potassium ferrioxalate actinometry (36). Experimental details of quantum yield calculation are given in the supporting information.

Single crystal X-ray analysis. The crystallographic data of (**3**) were collected using Mo-Kα radiation ($\lambda = 0.71073$ Å) using SMART APEX DUO diffractometer equipped with charge coupled device detector. Data were collected at room temperature. The data integration and reduction were carried out using SAINT-PLUS software. An empirical absorption correction was applied to the collected reflections with SADABS. The structure was solved by direct methods using SHELXS97 and refinement was carried out by full-matrix least-squares technique using SHELXL97. Anisotropic displacement parameters were calculated for all nonhydrogen atoms.

RESULTS AND DISCUSSION

Synthesis

The dienes (**1**–**6**) utilized in this investigation were synthesized by using Horner–Wadsworth–Emmons reaction (37) (Scheme 1a). In a typical procedure, triethyl phosphite (5.74 mmol) was added to the THF solution of *o*-, *m*- and *p*-nitrobenzyl bromide (2.3 mmol) and refluxed for 24 hours under N_2 atmosphere. The reaction mixture was first cooled to room temperature and then to 0°C using an ice bath. Sodium hydride (11.5 mmol) was added to this cooled mixture and allowed to stir for 5 minutes. Aldehyde (2.3 mmol) [*trans*-cinnamaldehye for (**1**–**3**) and *E* isomer of 3-pyridin-4-yl-propenal for (**4**–**6**)] was added drop wise and stirring was continued for an additional 30 minutes. The propenal derivative was synthesized using established literature procedures by a reaction of triphenylphosphoranylidene acetaldehyde and pyridine-4-carbaldehyde at room temperature (38) (Scheme 1b). Progress of the reaction was monitored using thin layer chromatography (TLC) and the reaction was quenched by adding water. The organic layer was extracted using dichloromethane and concentrated under reduced pressure. The crude reaction mixture so obtained was purified by column chromatography using silica gel as a stationary phase with 5–30% ethyl acetate in petroleum ether as eluent. Characterization spectra for all the synthesized products were given in the supplementary information.

Absorption

Diene (**1**) containing a nitro group at the *p*-position absorbs (λ_a) at ~377 nm in acetonitrile. In comparison, changing the position of the nitro group to *meta* (**2**) results in significant blueshifted (~47 nm) absorption. Furthermore, placing the nitro group in *ortho* (**3**) results in a greater hypsochromic shift (~61 nm). Dienes (**4**–**6**) also demonstrate a similar trend in their absorption properties. Nitro substitution at *m*- and *o*-positions leads to significant hypsochromic shifts, 37 nm for (**5**) and 52 nm for (**6**), as compared to *p*-substituted (**4**) which has absorption maxima at 363 nm in acetonitrile. In general, substitution of an electron withdrawing pyridyl ring in place of a phenyl ring yields a blueshifted absorption. The absorbance and fluorescence data of dienes are listed in Table 1. The observed order of absorption, *p*- > *m*- > *o*- is explained by mesomeric effects caused by changes in position of the nitro group. Among the dienes investigated, (**1**) exhibits the largest λ_a and *o*-substituted (**6**) the lowest (Fig. 2a). These hypsochromic shifts may be ascribed to the nonplanar interaction between the nitro and conjugated diene system hampering the delocalization. Upon changing the solvent polarity from heptane to dioxane or acetonitrile varying amounts (1–13 nm) of redshifts in absorption maxima were observed. The absorption spectrum is generally structured in nonpolar heptane, whereas structural features are less demarcated in polar solvents. These structural and absorption shifts are a result of increased solute–solvent interactions.

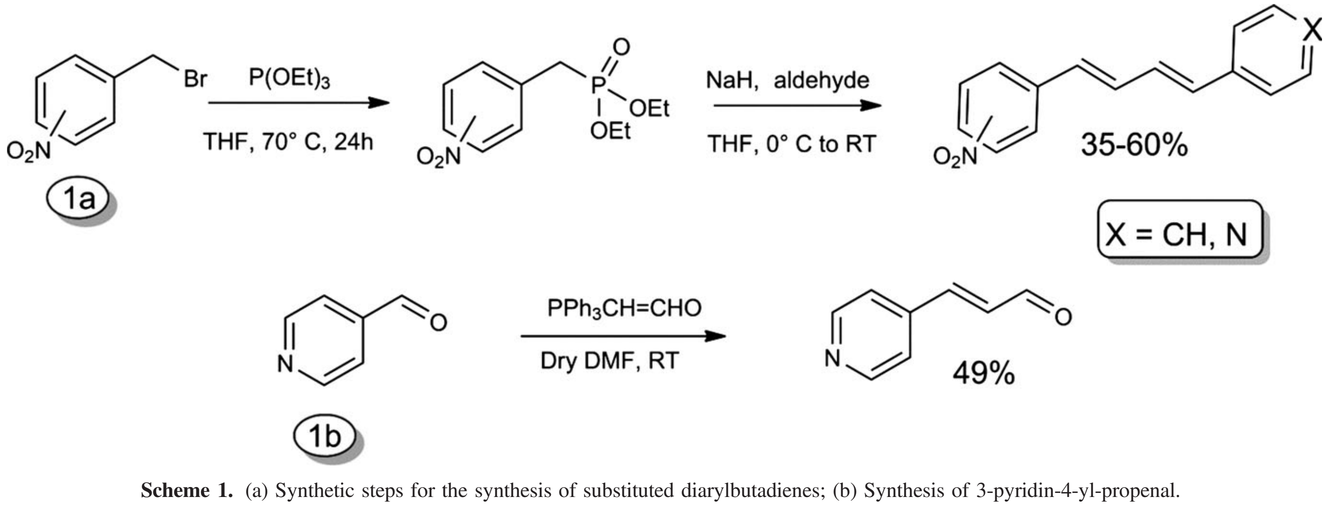

Scheme 1. (a) Synthetic steps for the synthesis of substituted diarylbutadienes; (b) Synthesis of 3-pyridin-4-yl-propenal.

Table 1. Absorption and fluorescence data of dienes (**1**–**6**) in homogeneous solvents.

	(**1**)			(**2**)			(**3**)		
Dienes	λ_a	λ_f	Φ_f*	λ_a	λ_f	Φ_f*	λ_a	λ_f	Φ_f*
Heptane	372	427	0.005	331	375	0.004	316	356	0.008
Dioxane	374	462	0.006	332	521	0.002	320	365, 413	0.001
THF	378	486	0.020	332	541	0.001	319	383	0.001
CH_3CN	377	560	0.114	330	–	0.001	316	365	0.001
DMF	385	560	0.171	333	–	0.001	320	368	0.002
	(**4**)			(**5**)			(**6**)		
Heptane	356	410	0.002	324	379	0.006	310	426	0.001
Dioxane	364	503	0.002	328	390, 503	0.001	315	433	0.001
THF	366	520	0.004	328	431, 499	0.001	316	434	0.001
CH_3CN	363	526	0.014	326	401, 572	–	311	434	0.001
DMF	372	521	0.020	327	384, 562	0.002	317	364	0.003

*Φ_f is determined using quinine sulfate (0.545 in 1N H_2SO_4 as a standard).

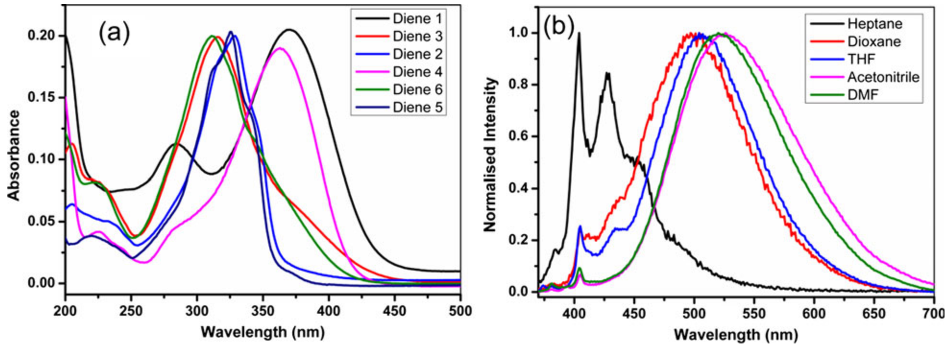

Figure 2. (a) UV–Vis absorption spectra of dienes (**1**–**6**) in acetonitrile; (b) Emission spectra of (**4**) in solvents of different polarity.

Molecular geometry and crystal structure

The *ortho*-derivative (**3**) was crystallized in acetone and the crystal structure was elucidated by single X-ray diffraction. The compound crystallizes into the orthorhombic space group Pca21 with one molecule in the asymmetric unit. The summary of the crystal data is given in the Table S1 (ESI). The X-ray molecular structure is shown in Fig. 3. X-ray data reveal that the nitro-substituted phenyl group in (**3**) is slightly deviated from the plane of the diene system with a dihedral angle (C_3-C_4-C_7-C_8) of −175.5°. The dihedral angle of (N_1-O_1-C_3-C_4) and ∠C-H···O bond angle of (**3**) in the crystal were measured to be 38.1 and 119.7°, respectively (Fig. 3). The (C-H···O) distance of 2.236 Å in (**3**) indicates possibility of an intramolecular hydrogen bond between the oxygen of the nitro group and hydrogen of the proximal double bond.

Emission of dienes (1–6)

p-nitro-substituted diphenylbutadiene derivatives exhibit remarkable solvatochromism that was attributed to the presence of strong intramolecular charge transfer (ICT) states (25,39,40). As

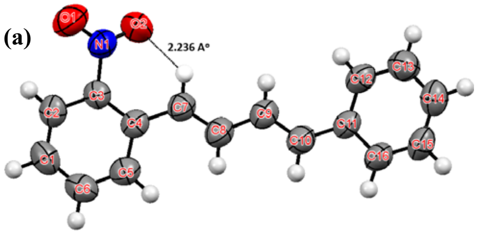

(b)	**Crystal (3)**
$\angle C_3 - C_4 - C_7 - C_8$	-175.5°
$\angle N_1 - O_1 - C_3 - C_4$	38.1°
$\angle C - H \ldots O$	119.7°
$(C - \mathrm{H} \cdots \mathrm{O})$	2.236 A°

Figure 3. (a) Intramolecular hydrogen bonding interaction; (b) Major geometrical parameters of the *ortho*-substituted diene obtained from the X-ray structure.

shown in Table 1, solvent polarity changes from heptane to acetonitrile result in significant a bathochromic emission shift (17), ~133 nm, for (**1**) (Fig. S1). Similar to (**1**), diene (**4**) also shows ICT characteristic emission (Fig. 2b). In both cases, the charge transfer excited state is greatly stabilized by the solvent resulting in a large redshifted emission. The greater sensitivity of fluorescence to solvent is also partly due to presence of twisted intramolecular charge transfer states (27).

In contrast to *para*-substituted dienes, *o*-nitro substitution results in very weak emission behavior for (**3**) and (**6**)**.** No ICT characteristic behavior was observed (Fig. S1). In these cases, the emission observed is merely due to locally excited state and changing the solvent does not affect the emission properties. The *ortho*-nitro group in (**3**) and (**6**) contribute to steric hindrance and also involve in favorable H-bonding interactions with proximal vinylene hydrogens. The geometries obtained from X-ray crystal data substantiate the presence of intramolecular C-H···O interactions in the ground state (Fig. 3). In contrast to this observation, both *m*-derivatives, despite the apparent loss in conjugation, show long wavelength intramolecular charge transfer band (ICT). Diene (**2**) gives dominant emission band in solvents of medium polarity such as THF and dioxane and quenched emission in acetonitrile and DMF (Fig. 4a). This emission is somewhat akin to that observed for *p*-substituted (**1** and **4**) where significant solvatochromism was observed. But in the case of (**5**), the CT band is very weak with emission bands at 500 nm in dioxane and 575 nm for acetonitrile along with bands in the higher energy region (Fig. S2). Sharp peaks at [~370 nm (**2, 5**) ~405 nm (**4**)] seen in emission spectra are due to Raman scattering peaks and are not characteristic of the compounds investigated. (These peaks were unavoidable despite using drier solvents and the intrinsic weak fluorescence of the dienes may also be a contributory factor.) The polarity dependent quenching of the emission is best illustrated using dioxane-acetonitrile binary mixture. Accordingly, as solvent polarity (% of acetonitrile) is increased, gradual redshifted emission is observed with concomitant quenching of fluorescence intensity (Fig. 4b). Solvent polarity also affects the fluorescence quantum yield. Fluorescence quantum yield (ϕ_f) is greater for medium polar solvents and decreases for solvents of higher polarity and is a result of competing radiationless decay pathways such as intersystem crossing (41). In general, the fluorescence quantum yield for all these investigated dienes is very low because of involvement of n-π* transitions of the pyridyl ring or competing decay processes due to nitro substitution.

Photoisomerization

Direct irradiation of diphenylbutadiene leads to formation of corresponding *cis* (*c*) and *trans (t)* isomers (42,43). In the case of unsymmetrically substituted diphenylbutadiene four isomers are technically possible, *trans-trans (tt)*, *trans-cis (tc)*, *cis-trans* (*ct*) and *cis-cis (cc)* isomers. But, it is established that suitably substituted diarylbutadienes upon irradiation yields highly selective isomerization products (34,44). In certain substitutions, such as *para*-substituted nitro diene (**1**), direct irradiation in acetonitrile leads to inefficient isomerization with about 2–4% formation of *cis* isomer despite prolonged irradiation (23). Similarly irradiation of (**4**) bearing an isoelectronic electron withdrawing pyridine ring in place of the phenyl ring also resulted in inefficient photoisomerization. Figure 5a displays the UV spectra of (**4**) at various time intervals of irradiation in acetonitrile and this result in a small decrease from 0.34 to about 0.30 absorbance units. The HPLC peak profiles before and after irradiation indicate only one predominant peak corresponding to the original *tt* isomer (Figs. S3a,b). NMR of the photomixture reveals no changes to the original NMR of *tt* spectra (Figs. 5b and S3c)**.** Despite presence of different electron withdrawing strengths at opposing ends (pyridine and nitrophenyl) the isomerization to the corresponding *cis-trans* isomer is almost nonexistent. Changing the position of the nitro group from *para* to *meta* (**2** & **5**) also do not yield any detectable photoproducts.

Such inefficient isomerization is not reported in similarly substituted nitrostilbenes (45,46). The UV–vis spectra of dienes (**2** and **5**) at various time intervals of irradiation, HPLC spectral details and NMR data of irradiated mixture are given in ESI (Figs. S4 and S5). Interestingly, the positional change in the nitro group to *ortho* (**3** & **6**) yields corresponding *cis* isomers. Absorption spectra of (**3**) & (**6**) indicate a gradual decrease in absorbance (Fig. 6a,b) with increase in time of irradiation. Clear isosbestic point indicates the presence of an equilibrating isomers and the observation was confirmed by HPLC peak profile of the photoirradiated mixture (Fig. S6). In contrast to *para-* or *meta*-substituted dienes, it is clear that *o*-substitution paves the path for easy isomerization. It is likely that the double bond closer to pyridine ring is the preferred site of isomerization (34) as substantiated by NMR studies (*vide infra*).

To confirm this, *trans-cis (tc)* isomer of (**3**) was isolated and characterized using absorption spectroscopy and NMR. UV spectra of *tc* isomer shows a blueshift of ~9 nm, with respect to *tt* (Fig. 6c), as a consequence of reduction in conjugation due to

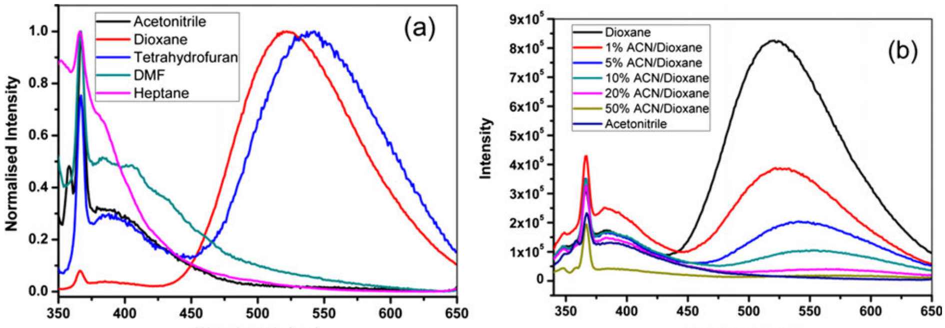

Figure 4. (a) Normalized emission spectra of diene (**2**) in varying solvent polarity; (b) in acetonitrile (ACN)/dioxane binary mixture.

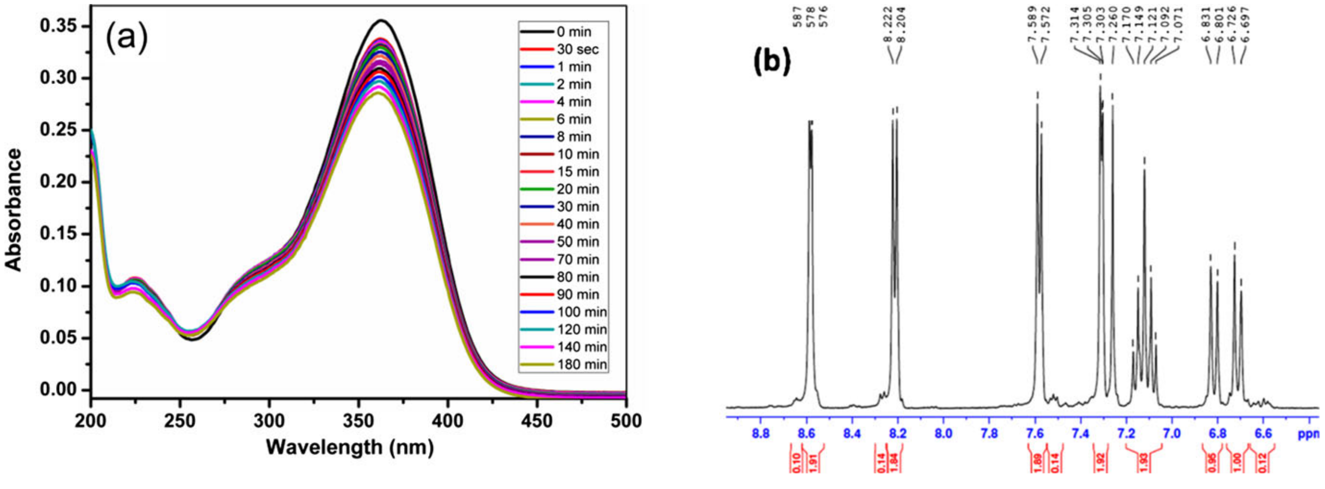

Figure 5. (a) UV spectral changes of diene (**4**) upon irradiation; (b) Photomixture NMR of diene (**4**) after irradiation.

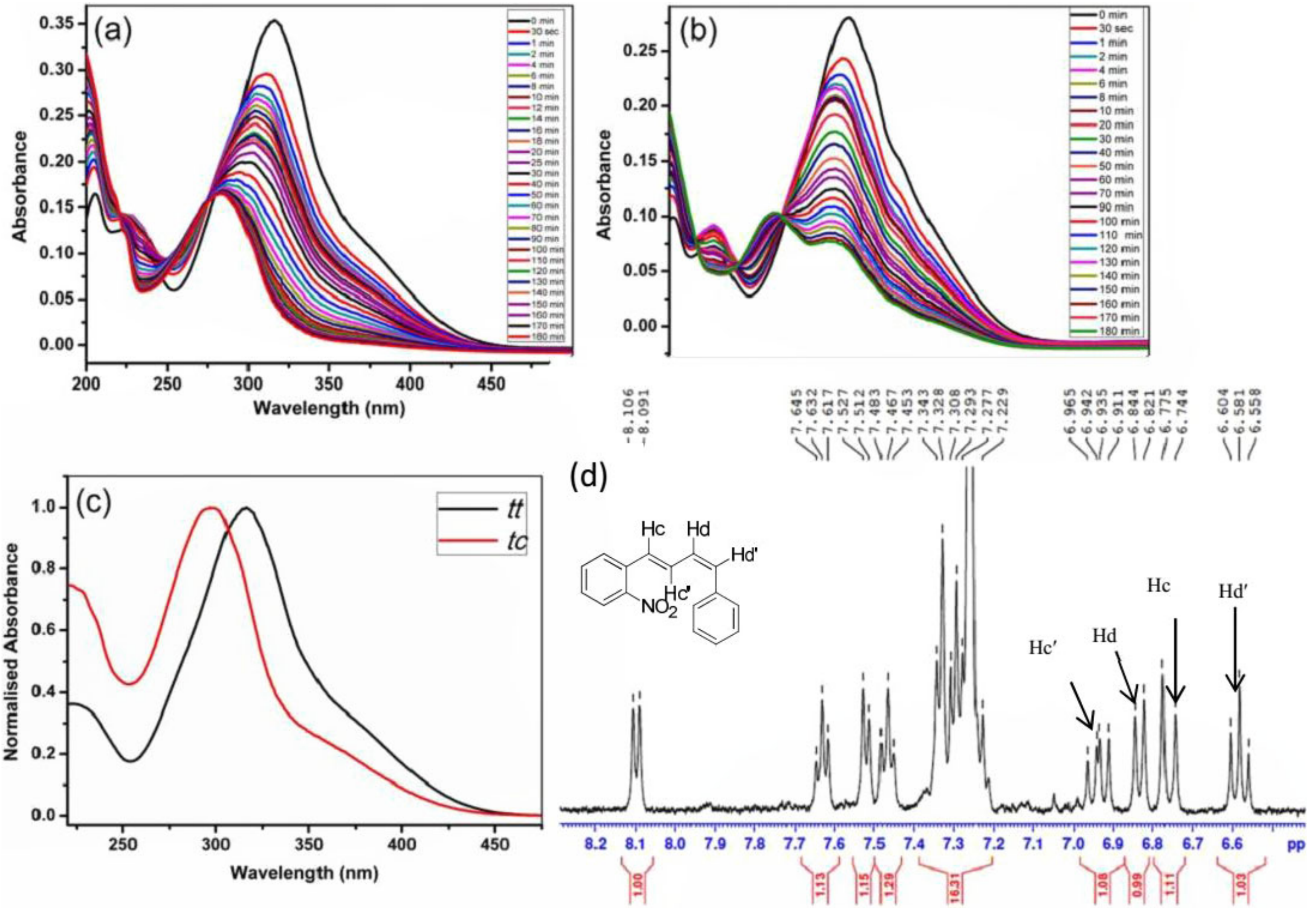

Figure 6. UV–vis absorption spectral changes upon irradiation of (a) diene (**3**) and (b) diene (**6**) in acetonitrile at various time intervals. (c) Comparative UV spectra of pure *trans* (black line) and cis (red-line) isomers of diene-**3**. (d) ^{1}H NMR spectra of *cis*-**3** in CDCl$_3$.

nonplanarity. The NMR spectra of pure *tc* isomer was also obtained by preparative TLC (5% ethylacetate/petroleum ether) and shown in Fig. 6d. The up-field shifting of chemical shift confirms that *trans* double bond far to nitro group converts to *cis*. Detailed NMR analysis reveals coupling constants 11.5 Hz for H$_d$ & H$_{d'}$ protons and 15.5 Hz for H$_c$ and H$_{c'}$ hydrogens. The values clearly indicate that only one of the double bonds retains its *trans* configuration. Table 2 gives comparative NMR values and their coupling constants of both the dienes (**3**) and (**6**). The peak at δ 6.77–6.74 of *tt* isomer merged with *tc* isomer. To observe a clear pattern, time dependent irradiation of (**3**) in CDCl$_3$ (3 mg/1 mL) was performed followed by NMR characterization which reveals the emergence of new isomer peaks (Fig. S7). We have further verified the formation of isomers using COSY spectral analysis. COSY spectra (Fig. S8) of irradiated (**3**) showed three cross peaks (A, B + B' and C). COSY spectra of *tc* isomer showed two cross peaks (B + C). The A and B cross peaks (squares) formed due to the interaction between hydrogens of *tt* isomer. The B′ cross peak display the interaction between hydrogens of *trans* configuration (Hc and Hc′) of *tc* isomer. The C cross peak display the interaction between hydrogens of *cis* configuration (Hd and Hd′) of *tc* isomer.

Similar to (**3**), pyridine containing diene (**6**) also undergoes facile isomerization and the position of isomerization is closer to the pyridyl group. The coupling constant observed (for **6**) was J = 11.0–11.5 Hz indicating *cis* coupling between protons. Figure S9 shows irradiation dependent time progression NMR spectra of (**6**) in $CDCl_3$ and reveal formation of new isomer peaks. The NMR of the photomixture, COSY spectra, mass spectral data for (**6**) are given in supplementary information (Figs. S10 and S11). We were unable to isolate the pure-*cis* component of (**6**) from the photomixture. The quantum yield of photoisomerization (ϕ_{PI}) obtained for the *ortho*-substituted dienes is also listed in Table 2. There is no significant trend observed upon changing the solvent polarity on ϕ_{PI}.

Preferential isomerization in *o*-substituted derivatives can be due to two reasons. First, possibility of intramolecular H-bond formation between nitro group and hydrogen of the precedent double bond, and second the possible involvement of zwitterionic intermediates. In the first case, the H-bond may impart steric congestion and structural rigidity to the system and this H-bonding decelerates the nonradiative processes to some extent leading to an isomerized product. The C-H···O Interactions, although relatively weak, play a decisive role in structural properties (47,48). Even though nitro group may experience steric repulsion with the double bond (49), single X-ray data reveal that the interaction between nitro group and hydrogen of the precedent double bond is quite high which may be predominant than the steric repulsion. As a consequence of this (C-H···O) interaction, *ortho* derivatives are more stable and also enable free rotation of the other double bond facilitating regioselective isomerization.

Although the electrostatic interactions involving the vinylene hydrogen and the nitro group may play a crucial role, we also envisage involvement of highly polarized zwitterionic excited states in imparting the regioselectivity (50–53) for *ortho*-isomers (Scheme 2). In this pathway, presence of strong electron withdrawing nitro group enables formation of zwitterionic canonical cationic intermediates (**3a**). Zwitterionic (**3a**) may lead to formation of a cyclical intermediate (**3b**) causing clear constraints for the isomerization and dictating the isomerization product at the phenyl (**3**) or pyridyl (**6**) side of the double bond. However, our experiments using time dependent NMR of the dienes (Figs. S7 and S9) under irradiation doesn't detect formation of

Table 2. Comparative NMR values and their coupling constants of dienes (**3**) and (**6**).

Diene	*trans-trans (tt)*	Photomixture	*trans-cis (tc)*	Solvent	ϕ_{PI}
3	δ 7.18–7.15 (d, 1H, J = 14.0 Hz), 7.03–6.94 (m, 2H), 6.77–6.74 (d, 1H, J = 15.0 Hz).	δ 7.18–7.15 (d, 14.5 Hz *tt*), δ 7.04–6.91 (m, *tt*, *tc*), δ 6.84– 6.82 (d, J = 11.5 Hz *tc*), δ 6.77– 6.74 (d, J = 15.5 Hz *tt*), δ 6.60–6.55 (t, 11.5 Hz *tc*)	δ 6.96–6.91 (m, J = 15.5 Hz), 6.84–6.82 (d, J = 11.5 Hz), 6.77–6.74 (d, J = 15.5 Hz), 6.60–6.55 (t, 11.5 Hz).	Dioxane CH_3CN	0.145 0.144
6	δ 7.20–7.15 (m, 1H, J = 15.5 Hz), 6.96–6.91 (m, 1H, J = 15.5 Hz), 6.68–6.65 (d, 1H, J = 15.5 Hz)	δ 7.20–7.15 (m, tt), 7.10–7.04 (m, J = 15.5 Hz, *tc*), 6.99–6.92 (m, *tt*, *tc*), 6.68–6.65 (d, J = 15.5 Hz, *tt*), 6.61–6.57 (t, J = 11.0 Hz, *tc*)	δ 7.10–7.04 (m, J = 15.5 Hz), δ 6.99–6.94 (d, J = 11.5 Hz), δ 6.68–6.65 (d, 15.5 Hz), 6.61–6.57 (t, J = 11.0 Hz).	Dioxane CH_3CN	0.15 0.14

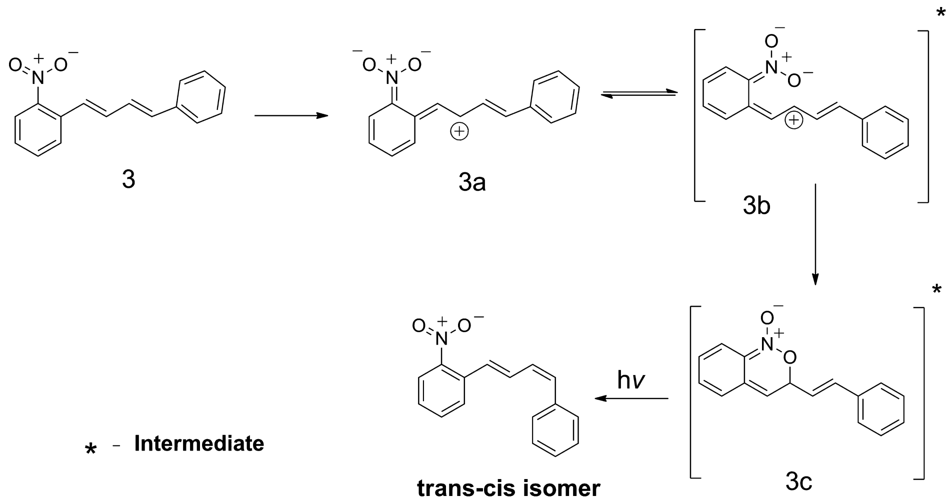

Scheme 2. Plausible mechanistic pathway to explain regioselective isomerization of *ortho* derivatives.

any cyclical intermediates. We assume that the time scale of their formation may be too small to be detected by using NMR. Thus, in these systems, interplay of electrostatic interactions through highly polarized zwitterionic excited states and (C-H···O) interactions directs the regioselective isomerization product.

CONCLUSIONS

The fluorescence and photochemical behavior of the *meta* isomers resemble that of the *para* isomers although significant absorption changes are detected upon change in the position of nitro substitution. In addition, *o*-nitro substitution induces greater photochemical reactivity than *para*- and *meta*-substituted compounds. X-ray crystal data analysis reveals possibility of intramolecular hydrogen bonding between oxygen of *ortho*-substituted NO_2 moiety with the proximal hydrogen of the vinylene bond. NMR spectroscopic observations clearly show preferential isomerization of the double bond that is in proximity to the pyridyl or the unsubstituted phenyl ring in *ortho*-dienes.

Acknowledgements—Authors gratefully acknowledge Council of Scientific and Industrial Research (CSIR), Department of Science and Technology (DST) and IIT Gandhinagar for financial support. Acknowledgements are also due to Dr. Darshak Trivedi and Mr. Bharat Kumar, NIT Surathkal for their help in recording single crystal X-ray data.

SUPPORTING INFORMATION

Additional Supporting Information may be found in the online version of this article:

Table S1. Crystallographic data for diene (**3**).

Figure S1. Normalized emission spectra of dienes (**1**) (**3**) and (**6**) in solvents of varying solvent polarity. Dienes-3 and 6 show weak emission profile and the sharp emission lines are due to Raman Scattering peaks.

Figure S2. Normalized emission spectra of diene (**5**) in solvents of varying solvent polarity.

Figure S3. (a) HPLC peak profile of diene (**4**) before and (b) after irradiation obtained using 370 nm as detection wavelength. (c) ^{1}H NMR spectra of diene (**4**) before irradiation.

Figure S4. (a) UV–Vis absorption spectrum upon irradiation of diene (**2**) in acetonitrile at different time intervals. HPLC peak profile of diene (**2**) (b) before and (c) after irradiation. ^{1}H NMR spectra of diene (**2**) (d) before irradiation and (e) after irradiation.

Figure S5. (a) UV–Vis absorption spectrum upon irradiation of diene (**5**) in acetonitrile at different time intervals. (b) HPLC peak profile before and after irradiation obtained using 330 nm as detection wavelength; (c) ^{1}H NMR spectra before irradiation and (d) ^{1}H NMR spectra after irradiation of diene (**5**).

Figure S6. HPLC Peak profiles of (**c**) diene (**3**) and (**d**) diene (**6**) after irradiation.

Figure S7. Time-dependent NMR study of (**3**) in $CDCl_3$ at different time intervals.

Figure S8. ^{1}H NMR (**3**) (a) before irradiation and (b) after irradiation. COSY spectra (c) after irradiation (mixture of *tt* and *tc*) and (d) of pure *tc* isomer.

Figure S9. Time-dependent irradiation of diene (**6**) in $CDCl_3$ at different time intervals.

Figure S10. ^{1}H NMR spectra of diene (**6**) (a) before irradiation and (b) after irradiation. COSY spectra (c) before irradiation and (d) after irradiation.

Figure S11. LCMS chromatogram and mass spectra of diene **6** after irradiation.

Appendix S1. Procedure for Quantum yield measurement.

Appendix S2. checkCIF/PLATON report.

REFERENCES

1. Wald, G. (1968) The molecular basis of visual excitation. *Nature* **219**, 800–807.
2. Rando, R. R. (1990) The chemistry of vitamin A and vision. *Angew. Chem. Int. Ed.* **29**, 461–480.
3. Jung, Y. O., J. H. Lee, J. Kim, M. Schmidt, K. Moffat, V. Srajer and H. Ihee (2013) Volume-conserving trans-cis isomerization pathways in photoactive yellow protein visualized by picosecond X-ray crystallography. *Nat. Chem.* **5**, 212–220.
4. Allen, M. T. and D. G. Whitten (1989) The photophysics and photochemistry of. α, ω-diphenylpolyene singlet states. *Chem. Rev.* **89**, 1691–1702.
5. Schapiro, I., O. Weingart and V. Buss (2008) Bicycle-pedal isomerization in a rhodopsin chromophore model. *J. Am. Chem. Soc.* **131**, 16–17.
6. Yang, L.-Y., R. S. H. Liu, K. J. Boarman, N. L. Wendt and J. Liu (2005) New aspects of diphenylbutadiene photochemistry. Regiospecific hula-twist photoisomerization. *J. Am. Chem. Soc.* **127**, 2404–2405.
7. Fuß, W. (2012) Hula-twist cis–trans isomerization: the role of internal forces and the origin of regioselectivity. *J. Photochem. Photobiol., A Chem.* **237**, 53–63.
8. Redwood, C. E., S. Kanvah, R. Samudrala and J. Saltiel (2013) Bicycle pedal photoisomerization of 1-phenyl-4-(4-pyridyl)-1,3-butadienes in glassy isopentane at 77 K. *Photochem. Photobiol. Sci.* **12**, 1754–1760.
9. Saltiel, J., M. A. Bremer, S. Laohhasurayotin and T. S. R. Krishna (2008) Photoisomerization of cis, cis- and cis, trans- 1,4-di-o-tolyl-1,3-butadiene in glassy media at 77 K: one-bond-twist and bicycle-pedal mechanisms. *Angew. Chem. Int. Ed.* **47**, 1237–1240.
10. Palakollu, V. and S. Kanvah (2014) Diphenylpolyene-cholesterol conjugates as fluorescent probes for microheterogeneous media. *J. Photochem. Photobiol. A Chem.* **281**, 18–26.
11. Terenziani, F., G. D'Avino and A. Painelli (2007) Multichromophores for Nonlinear Optics: designing the Material Properties by Electrostatic Interactions. *ChemPhysChem* **8**, 2433–2444.
12. Gao, X., T. Friscic and L. R. MacGillivray (2003) Supramolecular construction of molecular ladders in the solid state. *Angew. Chem. Int. Ed.* **43**, 232–236.
13. Abraham, S., R. K. Vijayaraghavan and S. Das (2009) Tuning microstructures in organogels: gelation and spectroscopic properties of mono- and bis-cholesterol-linked diphenylbutadiene derivatives. *Langmuir* **25**, 8507–8513.
14. Li, Y., T. Liu, H. Liu, M.-Z. Tian and Y. Li (2014) Self-assembly of intramolecular charge-transfer compounds into functional molecular systems. *Acc. Chem. Res.* **47**, 1186–1198.
15. El-Gezawy, H., W. Rettig and R. Lapouyade (2006) Solvatochromic behavior of donor-acceptor-polyenes: dimethylamino-cyano-diphenylbutadiene. *J. Phys. Chem. A* **110**, 67–75.
16. Di Cesare, N. and J. R. Lakowicz (2001) Wavelength-ratiometric probes for saccharides based on donor-acceptor diphenylpolyenes. *J. Photochem. Photobiol., A Chem.* **143**, 39–47.
17. Singh, A. K., M. Darshi and S. Kanvah (2000) α, ω-Diphenylpolyenes capable of exhibiting twisted intramolecular charge transfer fluorescence: a fluorescence and fluorescence probe study of nitro- and nitrocyano-substituted 1,4-diphenylbutadienes. *J. Phys. Chem. A* **104**, 464–471.
18. La Clair, J. J. (1997) Selective detection of the carbohydrate-bound state of concanavalin A at the single molecule level. *J. Am. Chem. Soc.* **119**, 7676–7684.

19. Alain, V., S. Redoglia, M. Blanchard-Desce, S. Lebus, K. Lukaszuk, R. Wortmann, U. Gubler, C. Bosshard and P. Gunter (1999) Elongated push-pull diphenylpolyenes for nonlinear optics: molecular engineering of quadratic and cubic optical nonlinearities via tuning of intramolecular charge transfer. *Chem. Phys.* **245**, 51–71.
20. Geskin, V. M., C. Lambert and J.-L. Bredas (2003) Origin of high second- and third-order nonlinear optical response in ammonio/borato diphenylpolyene zwitterions: the remarkable role of polarized aromatic groups. *J. Am. Chem. Soc.* **125**, 15651–15658.
21. Davis, R., N. S. S. Kumar, S. Abraham, C. H. Suresh, N. P. Rath, N. Tamaoki and S. Das (2008) Molecular packing and solid-state fluorescence of alkoxy-cyano substituted diphenylbutadienes: structure of the luminescent aggregates. *J. Phys. Chem. C* **112**, 2137–2146.
22. Skoric, I., I. Kikas, M. Kovacs, L. Fodor, Z. Marinic, K.i. Molcanov, B. Kojic-Prodic and O. Horváth (2011) Synthesis, photochemistry, and photophysics of butadiene derivatives: influence of the methyl group on the molecular structure and photoinduced behavior. *J. Org. Chem.* **76**, 8641–8657.
23. Agnihotri, H., V. Palakollu and S. Kanvah (2014) Selective photoisomerization of methyl substituted nitro diphenylbutadienes. *J. Photochem. Photobiol., A Chem.* **293**, 40–49.
24. Achelle, S., A. Barsella, C. Baudequin, B. Caro and F.o. Robin-le Guen (2012) Synthesis and photophysical investigation of a series of push–pull arylvinyldiazine chromophores. *J. Org. Chem.* **77**, 4087–4096.
25. Sonoda, Y., S. Tsuzuki, M. Goto, N. Tohnai and M. Yoshida (2009) Fluorescence spectroscopic properties of nitro-substituted diphenylpolyenes: effects of intramolecular planarization and intermolecular interactions in crystals. *J. Phys. Chem. A* **114**, 172–182.
26. Singh, A. K. and G. R. Mahalaxmi (2000) Excited state properties of α, ω-diphenylpolyenes: photophysical and photochemical studies of donor-acceptor diarylbutadienes. *Photochem. Photobiol.* **71**, 387–396.
27. Shin, D. M. and D. G. Whitten (1988) Solvatochromic behavior of intramolecular charge-transfer diphenylpolyenes in homogeneous solution and microheterogeneous media. *J. Phys. Chem.* **92**, 2945–2956.
28. Collado-Fregoso, E., J. S. Zugazagoitia, E. F. Plaza-Medina and J. Peon (2009) Excited-state dynamics of nitrated push– pull molecules: the importance of the relative energy of the singlet and triplet manifolds. *J. Phys. Chem. A* **113**, 13498–13508.
29. Carlotti, B., G. Consiglio, F. Elisei, C. G. Fortuna, U. Mazzucato and A. Spalletti (2014) Intramolecular charge transfer of push-pull pyridinium salts in the singlet manifold. *J. Phys. Chem. A* **118**, 3580–3592.
30. Bartocci, G., G. Galiazzo, U. Mazzucato and A. Spalletti (2001) Photophysics and photochemistry of the EE and ZE isomers of 1-(n-pyridyl)-4-phenyl-1,3-butadiene (n = 2, 3 and 4). *Phys. Chem. Chem. Phys.* **3**, 379–386.
31. Bartocci, G., G. Galiazzo, L. Latterini, E. Marri, U. Mazzucato and A. Spalletti (2002) Photoisomerization mechanisms and photoselectivity of the stereoisomers of 1-(pyrid-n-yl),4-phenylbuta-1,3-diene. *Phys. Chem. Chem. Phys.* **4**, 2911–2916.
32. Baraldi, I., A. Spalletti and D. Vanossi (2003) Rotamerism and electronic spectra of aza-derivatives of stilbene and diphenylbutadiene. A combined experimental and theoretical study. *Spectrochim. Acta A Mol. Biomol. Spectrosc.* **59A**, 75–86.
33. Mazzueato, U. and A. Spalletti (2003) Protonation effect on the excited state behavior of EE-1-(n-pyridyl)-4-phenylbutadienes (n = 2, 3 and 4). *Photochem. Photobiol. Sci.* **2**, 282–288.
34. Eastman, L. R. Jr, B. M. Zarnegar, J. M. Butler and D. G. Whitten (1974) Unusual case of selectivity in a photochemical reaction. Photoisomerization of unsymmetrical 1,3-dienes. *J. Am. Chem. Soc.* **96**, 2281–2283.
35. Russo, S. F. (1969) Two fluorescence experiments. *J. Chem. Educ.* **46**, 374.
36. Phillips, D. (1971) A quantitative photochemical experiment for undergraduates. *J. Chem. Educ.* **48**, 198.
37. Davis, R., S. Abraham, N. P. Rath and S. Das (2004) Observation of a non-conventional Horner–Wadsworth–Emmons olefination product and the effect of the lateral ethyl substitution on the solid state fluorescence. *New J. Chem.* **28**, 1368–1372.
38. van Loevezijn, A., J. Venhorst, W. I. Iwema Bakker, C. G. de Korte, W. de Looff, S. Verhoog, J.-W. van Wees, M. van Hoeve, R. P. van de Woestijne, M. A. W. van der Neut, A. J. M. Borst, M. J. P. van Dongen, N. M. W. J. de Bruin, H. G. Keizer and C. G. Kruse (2011) N'-(Arylsulfonyl)pyrazoline-1-carboxamidines as Novel, Neutral 5-Hydroxytryptamine 6 Receptor (5-HT6R) Antagonists with Unique Structural Features. *J. Med. Chem.* **54**, 7030–7054.
39. Singh, A. K., M. Darshi and S. Kanvah (1999) Twisted intramolecular charge transfer fluorescence in nitro-substituted [α],[ω]-diphenylpolyene compounds. *New J. Chem.* **23**, 1075–1078.
40. Yang, J.-S., C.-K. Lin, A. M. Lahoti, C.-K. Tseng, Y.-H. Liu, G.-H. Lee and S.-M. Peng (2009) Effect of ground-state twisting on the trans → cis photoisomerization and TICT state formation of aminostilbenes. *J. Phys. Chem. A* **113**, 4868–4877.
41. Görner, H. (1998) Photophysics and photochemistry of trans-4-nitrostilbenes and trans-2,4-dinitrostilbenes: effect of intramolecular charge transfer. *Ber. Bunsen. Physikal. Chem.* **102**, 726–737.
42. Pinckard, J. H., B. Wille and L. Zechmeister (1948) A comparative study of the three stereoisomeric 1, 4-diphenylbutadienes. *J. Am. Chem. Soc.* **70**, 1938–1944.
43. Yee, W. A., S. J. Hug and D. S. Kliger (1988) Direct and sensitized photoisomerization of 1, 4-diphenylbutadienes. *J. Am. Chem. Soc.* **110**, 2164–2169.
44. Liu, J., K. J. Boarman, N. L. Wendt and L. M. Cardenas (2005) Regiospecific photoisomerization of fluorinated (*E*, *E*)-1, 4-diphenyl-1, 3-butadienes. *Tetrahedron Lett.* **46**, 4953–4956.
45. Guesten, H. and L. Klasinc (1968) Quantum yields of the photochemical cis-trans isomerization of monosubstituted stilbenes. *Tetrahedron Lett.* **26**, 3097–3101.
46. Bent, D. V. and D. Schulte-Frohlinde (1974) Evidence for the triplet route in the photochemical trans.far. cis isomerization of nitrostilbenes in solution. *J. Phys. Chem.* **78**, 451–454.
47. Desiraju, G. R. (1996) The C-H…O hydrogen bond: structural implications and supramolecular design. *Acc. Chem. Res.* **29**, 441–449.
48. Desiraju, G. R. (2005) C-H…O and other weak hydrogen bonds. From crystal engineering to virtual screening. *Chem. Commun.*, **25**, 2995–3001.
49. Sonoda, Y., M. Goto, S. Tsuzuki and N. Tamaoki (2006) Fluorescence spectroscopic properties and crystal structure of a series of donor-acceptor diphenylpolyenes. *J. Phys. Chem. A* **110**, 13379–13387.
50. Jayathirtha Rao, V. (1994) Regioselective photoisomerization of dienes: role of polar excited state. *J. Photochem. Photobiol., A Chem.* **83**, 211–215.
51. Liu, R. S. H. and A. E. Asato (1984) Photochemistry and synthesis of stereoisomers of vitamin A. *Tetrahedron* **40**, 1931–1969.
52. Squillacote, M., J. Wang and J. Chen (2004) Electrostatic control of the regioselectivity in the photoisomerization of trans, trans-1-fluoro-2,4-hexadiene: evidence for competing conical intersections. *J. Am. Chem. Soc.* **126**, 1940–1941.
53. Squillacote, M. E. and T. C. Semple (1987) Polarization in the excited state of 1,3-pentadiene: experimental evidence for an allyl cation-methylene anion species. *J. Am. Chem. Soc.* **109**, 892–894.